Published in final edited form as:
J Orthop Res. 2009 August ; 27(8): . doi:10.1002/jor.20855.

Cartilage Abnormalities Associated with Defects of Chondrocytic Primary Cilia in Bardet-Biedl Syndrome Mutant Mice

Anjan P. Kaushik, B.S.[a,c], **James A. Martin, Ph.D.**[a], **Qihong Zhang, Ph.D.**[b], **Val C. Sheffield, M.D., Ph.D.**[b], and **Jose A. Morcuende, M.D., Ph.D.**[a,*]

[a]Department of Orthopaedic Surgery and Rehabilitation, University of Iowa

[b]Department of Pediatrics, University of Iowa

[c]University of Virginia School of Medicine

SUMMARY

Primary cilia are found on nearly every mammalian cell, including osteocytes, fibroblasts, and chondrocytes. However, the functions of primary cilia have not been extensively studied in these cells, particularly chondrocytes. Interestingly, defects in the primary cilium result in skeletal defects such as polydactyly in Bardet-Biedl Syndrome (BBS), a ciliary disorder that also results in obesity, retinopathy, and cognitive impairments (1–4). Wild-type mice and mutant mice of the ciliary proteins Bbs1, Bbs2, and Bbs6 were evaluated with respect to histological and biochemical differences in chondrocytes from articular cartilage and xiphoid processes. Using immunofluorescence microscopy, chondrocytic cilia were visualized from the load-bearing joints and non-load-bearing xiphoid processes. Significant differences in ciliary morphology were not identified between mutant and wild-type mice. However, after expanding chondrocytes in cell culture and implanting them in solid agarose matrix, it was seen that the fraction of ciliated cells in cultures from mutant mice was significantly lower than in the wild-type cultures ($p<.05$). In addition, in Safranin-O-stained whole joint sections, Bbs mutant mice had significantly lower articular joint thickness ($p<.05$) and lower proteoglycan content saturation ($p<.05$) than wild-type mice. Moreover, there were statistically significant differences of cell distribution between Bbs mutant and wild-type mice ($p<.05$), indicating that mutant articular cartilage had changes consistent with early signs of osteoarthritis. These data indicate that Bbs genes and their functions in the chondrocytic primary cilium are important for normal articular cartilage maintenance.

Keywords

chondrocyte; primary cilium; articular cartilage; Bardet-Biedl syndrome; osteoarthritis

INTRODUCTION

Primary cilia are unique organelles found on virtually every mammalian cell that play essential roles in vertebrate development, homeostasis, and sensory function. The specialized plasma membrane of the cilium contains a distinct array of receptors unique to the function of each cell. This membrane envelops the ciliary axoneme, which is made up of microtubules and associated proteins. Transport proteins carrying a multitude of distinct

*Corresponding Author, Correspondence: Jose A. Morcuende, Department of Orthopaedic Surgery, 200 Hawkins Drive, 01023 JPP, Iowa City, IA 52242, jose-morcuende@uiowa.edu, Phone: (319) 384-8041, Fax: (319) 353-7919.

receptors and signaling molecules run up and down the axoneme via the process of intraciliary transport (1–4).

Cilia have a wide morphological and functional spectrum in different tissues. Motile cilia contain dynein arms that allow sliding of adjacent microtubules, thereby generating motile force. These cilia have roles in respiratory mucociliary clearance, egg and sperm transport, and cerebrospinal fluid movement (1, 2, 4). Primary cilia lack dynein arms that allow motility; however, they have been found to be sensors of extracellular changes. Specialized sensory primary cilia are found in retinal photoreceptors, inner ear hair cells, and sensory neurons (1, 2, 5–9). In these cells primary cilia play fundamental cellular roles, particularly in membrane signal transduction.

Interestingly, most cells of the mammalian body, including osteocytes, fibroblasts, and chondrocytes, possess primary cilia (10, 11). To date, only a handful of studies have examined the chondrocytic primary cilium. Electron microscopy has shown that every chondrocyte has a single primary cilium (12–16). In the last few years, Poole et al. found that collagen fibers and proteoglycans around the chondrocyte influence ciliary orientation (11, 17), and that cilia are closely associated with the Golgi apparatus (11, 18). They proposed that the primary cilium acts as a “cellular cybernetic probe” that monitors the physicochemical state of the extracellular matrix (11). Supporting this hypothesis, Kouri et al. studied cartilage from patients with osteoarthritis (OA) and concluded that chondrocytes have motile elements that activate in response to OA damage (19, 20). Furthermore, Jensen et al. examined ciliary bending patterns using confocal microscopy and concluded that mechanical forces affect matrix molecules around the primary cilium (21). Finally, chondrocytic cilia have receptors for integrins and proteoglycans (22), indicating that these matrix molecules bind directly to the cilium and cause mechanical bending and mechanosensory input.

Recent studies using knockout mouse strains of ciliary proteins have described mice with polydactyly and shortened limbs, caused by errors in post-natal growth plate development (23–25). These mouse studies indicate that defects in ciliary proteins result in skeletal anomalies; therefore, the primary cilium likely has a profound role in chondrocytic function. These findings provide the rationale for this study, in which the investigators chose to examine chondrocytic cilia in Bardet-Biedl Syndrome (BBS), a pathological state caused, at least in part, by ciliary defects. BBS results in skeletal defects such as polydactyly, obesity, retinal dystrophy, mental retardation, renal abnormalities, and hypogenitalism. The syndrome involves at least 12 genes, each coding for unique BBS proteins. These proteins have been localized to cilia and appear to affect intraciliary transport (26–28). A stable complex consisting of seven of these proteins, known as the BBSome, appears to also be integral to ciliogenesis and vesicular transport to the cilium (29).

The objective of this study was to evaluate the effects in cartilage of mutations in primary cilia proteins by examining histological and biochemical differences between the joints of wild-type mice and those of three distinct BBS ciliary protein mutant mice. The mouse models used in this study included one BBS gene knockin ($Bbs1^{M390R/M390R}$), containing the most common human BBS mutation, and two BBS gene knockouts ($Bbs2^{-/-}$, $Bbs6^{-/-}$) (27, 30–32).

MATERIALS AND METHODS

Mouse Strains

All BBS mouse strains used in this study have been described in prior publications (3, 4, 14). Mouse strains are on a mixed genetic background of 129.SVEV × C57BL/6 Black 6

mice. $Bbs1^{M390R/M390R}$ is a knockin strain, in which the Bbs1 gene has been deleted from the genome and replaced with a mutated copy of the gene (30). The knockout strains $Bbs2^{-/-}$ (31) and $Bbs6^{-/-}$ (also known as $Mkks^{-/-}$ in the literature) (32) have deletions of their respective BBS genes. Wild-type Bbs1 littermates served as controls. All mice bred for this study were handled and sacrificed ethically, in accordance with animal care standards regulated by the Institutional Animal Care and Use Committee through the Office Of Animal Resources.

Immunofluorescence Microscopy Studies

Two adult mice aged 8–10 months from each mouse strain were used for immunofluorescence staining. Six load-bearing joints were dissected and examined from each mouse: 2 knees, 2 hips, and 2 shoulders. The xiphoid process was also studied and served as a non-load-bearing cartilage control. Joints were placed in Dulbecco's Phosphate Buffered Saline (PBS) and then frozen into blocks using cryosectioning gel in 2-methylbutane. These frozen blocks were serially sectioned from the center of each joint into 10um sections using a Minotome Plus Cryostat (IEC; Needham Heights, MA). After the sections were placed onto microscope slides and allowed to dry, they were placed in 10% Buffered Neutral Formalin (BNF). Further steps can be found in commonly utilized immunofluorescence protocols. Two primary antibodies were used to detect proteins that localize to the primary cilium: rabbit antibody to Polaris (1:500) and monoclonal mouse antibody to Acetylated α-Tubulin (1:4000) (Sigma-Aldrich; St. Louis, MO). Alexa-Fluor 488 goat anti-mouse and 568 goat anti-rabbit secondary fluorescent antibodies were prepared in a 1:1000 dilution (Invitrogen; Carlsbad, CA) and 4',6-diamidino-2-phenylindole (DAPI) was used to stain nuclei. Slides were mounted with Vectashield solution (Vector; Burlingame, CA) and cover slips to protect the fluorescence. Tissues were visualized using a BX-51 Fluorescence microscope (Olympus; Center Valley, PA), and images viewed at 20× and 40× magnification were stored digitally. Each 10um section was scanned serially through the complete thickness of the sample to detect cilia on chondrocytes three-dimensionally.

Histology studies

Forty-six (46) adult mice were used for the histological analysis: 17 $Bbs1^{M390R/M390R}$, 3 $Bbs2^{-/-}$, 3 $Bbs6^{-/-}$, and 23 littermate wild-type controls. Fewer $Bbs2^{-/-}$ and $Bbs6^{-/-}$ mice of appropriate age were available in the laboratory's mouse colonies; however, appropriately age-matched controls were used. The $Bbs1^{M390R/M390R}$ strain provided the greatest statistical power, but the other two strains also provided statistically significant results. Older mice aged 6 to 14 months were utilized in order to detect early signs of cartilage abnormalities in the knockin/knockout mice. The xiphoid process and both knee joints were dissected from each mouse and fixed in 10% BNF for two days and then decalcified in 5% formic acid for two more days. The tissues were then sequentially dehydrated, cleared, and infiltrated with hot paraffin overnight at 56°C. After the tissues were placed in blocks of heated paraffin and properly oriented for standardized sectioning, the blocks were cooled and allowed to solidify. To obtain consistent 5um sections, these paraffin blocks were serially sectioned using a paraffin microtome (Leica, Germany) from the center of each joint moving laterally. Sections were placed onto microscope slides for Safranin-O staining. Slides were dried in a 60°C oven and sequentially stained with Weigert's Hematoxylin, Fast Green FCF, and Safranin-O using a standard staining protocol. After the slides were washed in ethanol and xylene, they were mounted with Permount and cover slips. Tissues were visualized at 10× and 20× magnification using a BX-51 Optical microscope (Olympus; Center Valley, PA) and digitally stored for quantification and analysis.

Cell Culture studies

Nine (9) mice were used for cell culture and the agarose timecourse: 4 $Bbs1^{M390R/M390R}$, 1 $Bbs2^{-/-}$, 1 $Bbs6^{-/-}$, and 3 littermate wild-type controls. Cartilage was obtained from the xiphoid process and knee joints of each mouse. Scrapings of cartilage were placed in growth medium (450mL Dulbecco's modified eagle medium high glucose, 450mL Ham's F-12 medium, 100mL fetal bovine serum, 10mL amphotericin B, 5mL ciprofloxacin) and then digested with bacterial collagenase (0.5% w/v) at 37°C for 5 hours to release cells. Released chondrocytes were collected by centrifugation, placed in fresh growth medium, and grown for 3 weeks in monolayer culture. Medium was replaced every 2 days and cells were transferred to larger flasks when necessary. Total cell number was determined when cells were confluent by treating the cells with Hanks balanced salt solution and trypsin-EDTA, followed by Haemocytometer counting.

Cells were suspended at a density of 1×10^6 chondrocytes per 100uL agarose into a solution of heated 1% liquid agarose and placed into 5cm plastic cylinders of 6mm diameter. Placement in agarose allowed cells to maintain a chondrocytic phenotype rather than reverting to a fibroblastic phenotype, which can occur in extended monolayer culture. After the agarose solidified into a gel, the 5cm cylinders were placed in fresh growth medium and cut into 5mm plugs. One chondrocyte-agarose plug was frozen each day for 2 weeks using cryosectioning gel in 2-methylbutane. The frozen plugs were cut in 10um sections onto microscope slides that were used for immunofluorescence microscopy, which has been detailed above. During the cell growth and agarose preparation process, there was a minimum of 56 cultures obtained from each mouse. Images taken at 20× and 40× magnification were digitally stored and quantified.

Measurements and Statistical Analysis

All digital images were analyzed using Photoshop (Adobe; San Jose, CA) and ImageJ (NIH; Bethesda, MD). To ensure that data analysis was unbiased, all histological analysis was performed in a blinded manner. Four 20× Safranin-O stained images of the tibial plateaus from each mouse were systematically quantified for several variables: articular cartilage thickness, percent proteoglycan saturation, cell density (superficial, deep, total), and cell distribution (superficial to deep cell ratio).

Mean articular cartilage thickness (um) was calculated by averaging 6 equally spaced measurements of the distance from cartilage surface to subchondral bone on each 20× slide. Human articular cartilage is normally defined to have three zones; however, it was exceedingly difficult to distinguish three distinct zones in mice because of the reduced articular cartilage thickness and the paucity of cells in each 5um section. Therefore, the investigators chose to divide the articular cartilage into two equally sized zones: superficial layer and deep layer. The superficial layer was defined as the 50% of cartilage area (um^2) closest to the joint surface, and the deep layer was the remaining 50% of cartilage area (um^2) closest to subchondral bone. The lines separating the two layers and area calculations were made digitally using Adobe Photoshop. Mean proteoglycan saturation was determined by digitally measuring and averaging the Safranin-O red saturation hue at 6 equally spaced points in the superficial layer of articular cartilage on each 20× slide. Superficial cell density (cells/um^2) was defined as the number of total superficial layer cell counts divided by the superficial layer area. Deep cell density (cells/um^2) was calculated similarly using deep layer cell counts and area. Superficial to deep (S/D) cell ratios were determined by dividing superficial cell counts over deep cell counts.

From the agarose cultures, four immunofluorescence images from each day of the 2-week timecourse were analyzed for: total number of cells (y), number of ciliated cells (x), and

fraction of ciliated cells per 20× field of view (x/y). Each 10um section was scanned serially through the complete thickness of the sample for the presence of cilia on chondrocytes, to ensure the proper three-dimensional quantification of cilia. This method was more comprehensive than examining merely a two-dimensional profile of chondrocytic cilia. Images presented in this publication (Fig. 5) display sample two-dimensional profiles containing the greatest number of visible cilia in each section. Data were analyzed using Excel (Microsoft, Redmond, WA) and presented as mean ± standard error. Statistical significance was set at $p<0.05$ and determined using the comparison t-test for cartilage differences between wild-type and knockin/knockout mice.

RESULTS

Chondrocytic cilia were visualized with immunofluorescence microscopy using antibodies to Polaris and acetylated α-tubulin (Fig. 1). Cilia were visible in the xiphoid processes as well as articular cartilage and growth plate cartilage of shoulder, hip, and knee joints in every mouse strain. Acetylated α-tubulin co-localized with Polaris in >90% of chondrocytes visualized using serial three-dimensional imaging, confirming that the ciliary axoneme was properly identified. Although immunofluorescence microscopy allowed visualization of cilia, this technique did not detect gross morphological ciliary differences between Bbs mutant and wild-type mice.

Histological analysis of tibial plateaus with Safranin-O staining illustrated differences in articular cartilage morphology between wild-type and Bbs mutant mice (Fig. 2). There were differences in cell density and distribution, articular cartilage thickness, and proteoglycan density between wild-type and knockin/knockout mice. Quantification of these variables demonstrated that the superficial layer of $Bbs1^{M390R/M390R}$, $Bbs2^{-/-}$, and $Bbs6^{-/-}$ articular cartilage had similar cell density to wild-type cartilage (Fig. 4a), $p>0.05$), however, the cell density of $Bbs1^{M390R/M390R}$, $Bbs2^{-/-}$, and $Bbs6^{-/-}$ cartilage was significantly higher in the deep layer (Fig. 4b), $p<0.05$). This indicated a cell distribution abnormality in $Bbs1^{M390R/M390R}$, $Bbs2^{-/-}$, and $Bbs6^{-/-}$ tissues; therefore, the superficial to deep (S/D) cell ratio was determined. $Bbs1^{M390R/M390R}$, $Bbs2^{-/-}$, and $Bbs6^{-/-}$ articular cartilage had S/D cell ratios of 1.18 (54%S : 46%D), 1.23 (55%S : 45%D), and 1.10 (52%S : 48%D), respectively. These ratios were significantly lower than the $Bbs^{+/+}$ wild-type S/D ratio of 2.01 (66%S : 34%D) ($p<0.05$). In addition, $Bbs1^{M390R/M390R}$, $Bbs2^{-/-}$, and $Bbs6^{-/-}$ cartilage had significantly lower proteoglycan saturation (Fig. 3a), $p<0.05$) and thickness (Fig. 3b), $p<0.05$) than wild-type. The tissues from mutant Bbs mice were also consistently observed to have a more ragged joint contour with several small surface fibrillations, as seen in Fig. 2b–d). Additionally, thinning of the subchondral bone and chondrocytic clustering indicative of cloning were observed in $Bbs1^{M390R/M390R}$, $Bbs2^{-/-}$, and $Bbs6^{-/-}$ tissues, but not in wild-type tissues. These findings are consistent with signs of osteoarthritis (19, 20).

Chondrocytes cultured in agarose also demonstrated differences in cilia (Fig. 5). In every joint and xiphoid section examined three-dimensionally using serial immunofluorescence microscopy, Bbs mutant cultures (from $Bbs1^{M390R/M390R}$, $Bbs2^{-/-}$, and $Bbs6^{-/-}$ animals) had a significantly lower fraction of ciliated chondrocytes than wild-type on days 1, 4, 7, and 10 of culture ($p<0.05$ in all comparisons) (Fig. 6).

DISCUSSION

The primary cilium has been proposed to be a chemosensor and mechanosensor of extracellular fluid flow in several tissues, for example in the renal proximal tubule where cilia sense urinary flow (1, 7–9); therefore, chondrocytes could also use primary cilia as sensors of the physicochemical environment. Recent research on the chondrocytic primary

cilium suggests a sensory function (11, 17–22); however, a solid understanding of the sensory mechanisms for chemical and mechanical forces, downstream signaling, and effects on cellular function is still not well established. The basal body of the cilium is physiologically coupled to the nucleus and Golgi apparatus in chondrocytes (11, 18), which implies that synthetic and secretory function of extracellular matrix components may be controlled in part by the cilium. Collagen fibers, integrins, and proteoglycans have been found to influence the orientation of the cilium (17). Of note, the cilium has even been found to have receptors for integrins and proteoglycans that interact directly with the axoneme (22). Thus the evidence strongly suggests a significant role of the primary cilium in basic chondrocytic functioning.

The results of this study support the hypothesis that the chondrocytic primary cilium is an integral element to the maintenance of healthy cartilage. When compared to wild-type mice, $Bbs1^{M390R/M390R}$, $Bbs2^{-/-}$, and $Bbs6^{-/-}$ mice had significantly lower articular cartilage thickness and proteoglycan density, as well as an abnormal cell distribution and fibrillations at the joint surface. Statistical power was greatest in the $Bbs1^{M390R/M390R}$ mice (n=17). These substantial histological differences reveal that Bbs gene functions are likely necessary for sustaining extracellular matrix production in the articular cartilage and for preserving the integrity of the joint surface. Cell culture in agarose also found that $Bbs1^{M390R/M390R}$, $Bbs2^{-/-}$, and $Bbs6^{-/-}$ tissues have a significantly lower fraction of ciliated chondrocytes relative to wild-type tissues over time.

The abnormal appearance of Bbs knockin/knockout articular cartilage suggests two possibilities: either there are early signs of osteoarthritis (OA), or Bbs affected mice never developed healthy articular cartilage even at a young age. When examining human osteoarthritic cartilage, Kouri et al. noted that aside from the obvious fibrillations at the joint surface, the cell distribution changed at higher stages of OA: morphologically different types of chondrocytes became more randomly dispersed within the articular cartilage layers, and superficial and deep layers were less distinguishable (19, 20). Those findings agree with this study's histological observations in Bbs mutant tissues. The low S/D ratios in $Bbs1^{M390R/M390R}$, $Bbs2^{-/-}$, and $Bbs6^{-/-}$ articular cartilage demonstrate a random dispersal of cells and a poorly distinguishable border between superficial and deep layers. Wild-type cartilage had a more evident superficial layer with a high saturation of proteoglycans and high cell density, whereas the deep layer had a lower cell density.

Alternatively, it is possible that Bbs mutant mice never formed healthy articular cartilage during development. Recent research strongly suggests that cartilage development in ciliary knockout mice is affected at early developmental stages. For example, mice with Polaris/Ift88/Tg737 and Kif3a conditionally knocked out in cartilage showed skeletal abnormalities resulting from abnormal Indian hedgehog and Sonic hedgehog signaling, as well as growth plate abnormalities from failure of chondrocyte rotation (23, 24). Similar post-natal growth plate defects were seen in transgenic mice with Polaris gene mutations (25). Therefore, a future study of cartilage in Bbs knockin/knockout mice during early developmental stages is needed to investigate signaling and functional deficiencies in the chondrocytic primary cilium.

The optical imaging of chondrocytic cilia using a conventional fluorescence microscope was a limitation to this study. The accuracy of this method for examining cells serially is inferior to that of a confocal microscope. Cells at the edges of each 10um section may have had cilia in adjacent sections, so this can account for some error in estimation of ciliary incidence. The researchers recommend the use of confocal microscopy in future studies examining chondrocytic cilia with fluorescent markers. Another limitation was that the investigators used different numbers of mice from different mouse strains. However, appropriate age-

matched controls were used, and there were enough $Bbs1^{M390R/M390R}$ strain mice to provide adequate statistical power.

The quantitative cartilage differences noted in this study may also reflect a qualitative or functional difference. Mechanical sensation in articular cartilage may be deficient when chondrocytes have defective cilia; therefore, the direction of study can now be geared toward understanding the potential mechanosensory function of chondrocytic cilia. The investigators are currently examining the effect of biomechanical stress on Bbs knockin/knockout chondrocytes using a micropressure loading device to determine loading-induced changes in ciliary orientation, extracellular matrix production, and calcium fluxes.

This study supports the hypothesis that BBS genes involved in chondrocytic ciliary function play a significant role in the proper functioning of chondrocytes in cartilage. The information gathered here adds to the growing field of ciliary research, and the results may serve to better understand how the chondrocyte senses factors in the extracellular matrix.

Acknowledgments

The authors thank A. Ferguson, M. Andrews, G. Kurriger, and B. Laughlin for technical assistance. This study was funded, in part, by NIH grants R01-EY11298 and R01-EY17168 (to VCS) and the University of Iowa Doris Duke Clinical Research Fellowship program (to APK). VCS is an investigator of the Howard Hughes Medical Institute.

REFERENCES

1. Rosenbaum JL, Witman GB. Intraflagellar transport. Nat Rev Mol Cell Biol. 2002; 3:813–825. [PubMed: 12415299]
2. Sloboda RD. Intraflagellar transport and the flagellar tip complex. J Cell Biochem. 2005; 94:266–272. [PubMed: 15558569]
3. Piperno G, Siuda E, Henderson S, Segil M, Vaananen H, Sassaroli M. Distinct mutants of retrograde intraflagellar transport (IFT) share similar morphological and molecular defects. J Cell Biol. 1998; 143:1591–1601. [PubMed: 9852153]
4. Pazour GJ, Rosenbaum JL. Intraflagellar transport and cilia-dependent diseases. Trends Cell Biol. 2002; 12:551–555. [PubMed: 12495842]
5. Pazour GJ, Baker SA, Deane JA, Cole DG, Dickert BL, Rosenbaum JL, Witman GB, Besharse JC. The intraflagellar transport protein, IFT88, is essential for vertebrate photoreceptor assembly and maintenance. J Cell Biol. 2002; 157:103–113. [PubMed: 11916979]
6. Praetorius HA, Spring KR. Bending the MDCK cell primary cilium increases intracellular calcium. J Membr Biol. 2001; 184:71–79. [PubMed: 11687880]
7. Praetorius HA, Spring KR. A physiological view of the primary cilium. Annu Rev Physiol. 2005; 67:515–529. [PubMed: 15709968]
8. Davenport JR, Yoder BK. An incredible decade for the primary cilium: a look at a once-forgotten organelle. Am J Physiol Renal Physiol. 2005; 289:F1159–F1169. [PubMed: 16275743]
9. Pazour GJ, Witman GB. The vertebrate primary cilium is a sensory organelle. Curr Opin Cell Biol. 2003; 15:105–110. [PubMed: 12517711]
10. Whitfield JF. Primary cilium--is it an osteocyte's strain-sensing flowmeter? J Cell Biochem. 2003; 89:233–237. [PubMed: 12704786]
11. Poole CA, Flint MH, Beaumont BW. Analysis of the morphology and function of primary cilia in connective tissues: a cellular cybernetic probe? Cell Motil. 1985; 5:175–193. [PubMed: 4005941]
12. Meier-Vismara E, Walker N, Vogel A. Single cilia in the articular cartilage of the cat. Exp Cell Biol. 1979; 47:161–171. [PubMed: 467766]
13. Wilsman NJ. Cilia of adult canine articular chondrocytes. J Ultrastruct Res. 1978; 64:270–281. [PubMed: 712881]
14. Wilsman NJ, Farnum CE, Reed-Aksamit DK. Incidence and morphology of equine and murine chondrocytic cilia. Anat Rec. 1980; 197:355–361. [PubMed: 7436010]

15. Hart JAL. Cilia in articular cartilage. J Anat. 1968; 103:222.
16. Scherft J, Daems W. Single cilia in chondrocytes. J Ultrastruct Res. 1967; 19:546–555. [PubMed: 6055783]
17. Poole CA, Zhang ZJ, Ross JM. The differential distribution of acetylated and detyrosinated alpha-tubulin in the microtubular cytoskeleton and primary cilia of hyaline cartilage chondrocytes. J Anat. 2001; 199:393–405. [PubMed: 11693300]
18. Poole CA, Jensen CG, Snyder JA, Gray CG, Hermanutz VL, Wheatley DN. Confocal analysis of primary cilia structure and colocalization with the Golgi apparatus in chondrocytes and aortic smooth muscle cells. Cell Biol Int. 1997; 21:483–494. [PubMed: 9451805]
19. Kouri JB, Arguello C, Luna J, Mena R. Use of microscopical techniques in the study of human chondrocytes from osteoarthritic cartilage: an overview. Microsc Res Tech. 1998; 40:22–36. [PubMed: 9443154]
20. Kouri JB, Jimenez SA, Quintero M, Chico A. Ultrastructural study of chondrocytes from fibrillated and non-fibrillated human osteoarthritic cartilage. Osteoarthritis Cartilage. 1996; 4:111–125. [PubMed: 8806113]
21. Jensen CG, Poole CA, McGlashan SR, Marko M, Issa ZI, Vujcich KV, Bowser SS. Ultrastructural, tomographic and confocal imaging of the chondrocyte primary cilium in situ. Cell Biol Int. 2004; 28:101–110. [PubMed: 14984755]
22. McGlashan SR, Jensen CG, Poole CA. Localization of extracellular matrix receptors on the chondrocyte primary cilium. J Histochem Cytochem. 2006; 54:1005–1014. [PubMed: 16651393]
23. Song B, Haycraft CJ, Seo HS, Yoder BK, Serra R. Development of the post-natal growth plate requires intraflagellar transport proteins. Dev Biol. 2007; 305:202–216. [PubMed: 17359961]
24. Haycraft CJ, Zhang Q, Song B, Jackson WS, Detloff PJ, Serra R, Yoder BK. Intraflagellar transport is essential for endochondral bone formation. Development. 2007; 134:307–316. [PubMed: 17166921]
25. McGlashan SR, Haycraft CJ, Jensen CG, Yoder BK, Poole CA. Articular cartilage and growth plate defects are associated with chondrocyte cytoskeletal abnormalities in Tg737(orpk) mice lacking the primary cilia protein polaris. Matrix Biol. 2007; 26:234–246. [PubMed: 17289363]
26. Beales PL. Lifting the lid on Pandora's box: the Bardet-Biedl syndrome. Curr Opin Genet Dev. 2005; 15:315–323. [PubMed: 15917208]
27. Mykytyn K, Sheffield VC. Establishing a connection between cilia and Bardet-Biedl Syndrome. Trends Mol Med. 2004; 10:106–109. [PubMed: 15106604]
28. Yen HJ, Tayeh MK, Mullins RF, Stone EM, Sheffield VC, Slusarski DC. Bardet-Biedl syndrome genes are important in retrograde intracellular trafficking and Kupffer's vesicle cilia function. Hum Mol Genet. 2006; 15:667–677. [PubMed: 16399798]
29. Nachury MVLA, Zhang Q, Westlake CJ, Peränen J, Merdes A, Slusarski DC, Scheller RH, Bazan JF, Sheffield VC, Jackson PK. A core complex of BBS proteins cooperates with the GTPase Rab8 to promote ciliary membrane biogenesis. Cell. 2007; 129(6):1201–1213. [PubMed: 17574030]
30. Davis R, Sheffield VC. Manuscript in preparation.
31. Nishimura DY, Fath M, Mullins RF, Searby C, Andrews M, Davis R, Andorf JL, Mykytyn K, Swiderski RE, Yang B, Carmi R, Stone EM, Sheffield VC. Bbs2-null mice have neurosensory deficits, a defect in social dominance, and retinopathy associated with mislocalization of rhodopsin. Proc Natl Acad Sci U S A. 2004; 101:16588–16593. [PubMed: 15539463]
32. Fath MA, Mullins RF, Searby C, Nishimura DY, Wei J, Rahmouni K, Davis RE, Tayeh MK, Andrews M, Yang B, Sigmund CD, Stone EM, Sheffield VC. Mkks-null mice have a phenotype resembling Bardet-Biedl syndrome. Hum Mol Genet. 2005; 14:1109–1118. [PubMed: 15772095]

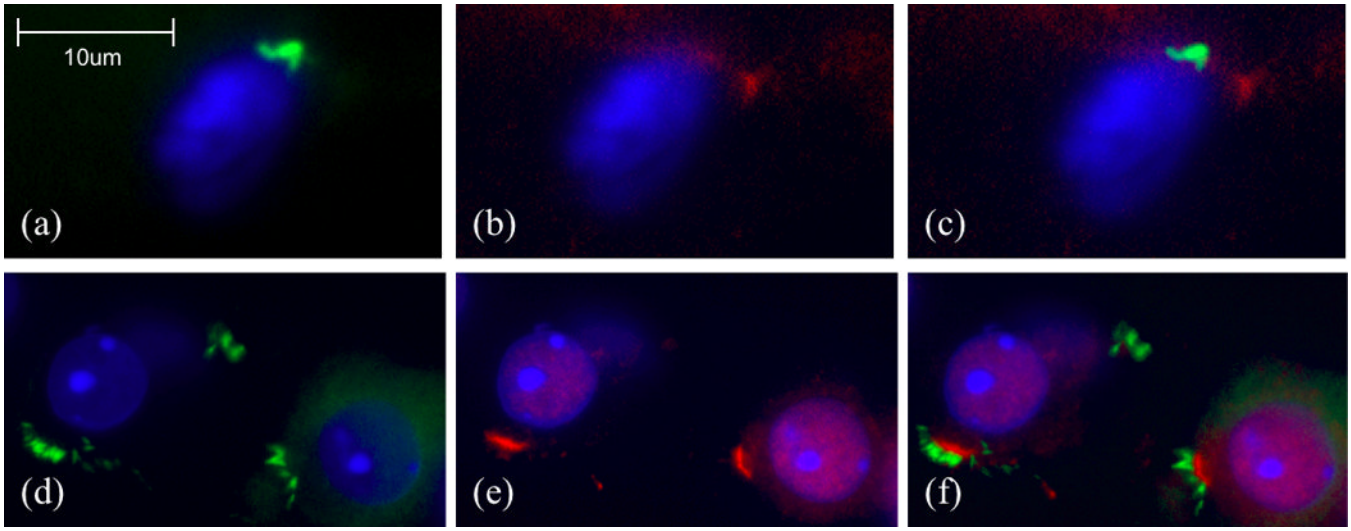

Fig. 1.

Immunofluorescence microscopy of chondrocytic cilia: (a–c) wild-type; (d–f) Bbs6$^{-/-}$. Images (a) and (d) display staining with DAPI nuclear marker (blue) and antibody to acetylated α-tubulin (green); (b) and (e) display DAPI with antibody to polaris (red); and (c) and (f) merge all three fluorescent markers. Co-localization of both ciliary proteins, acetylated α-tubulin and polaris, was observed. Bbs1$^{M390R/M390R}$ and Bbs2$^{-/-}$ are not shown but demonstrated similar properties.

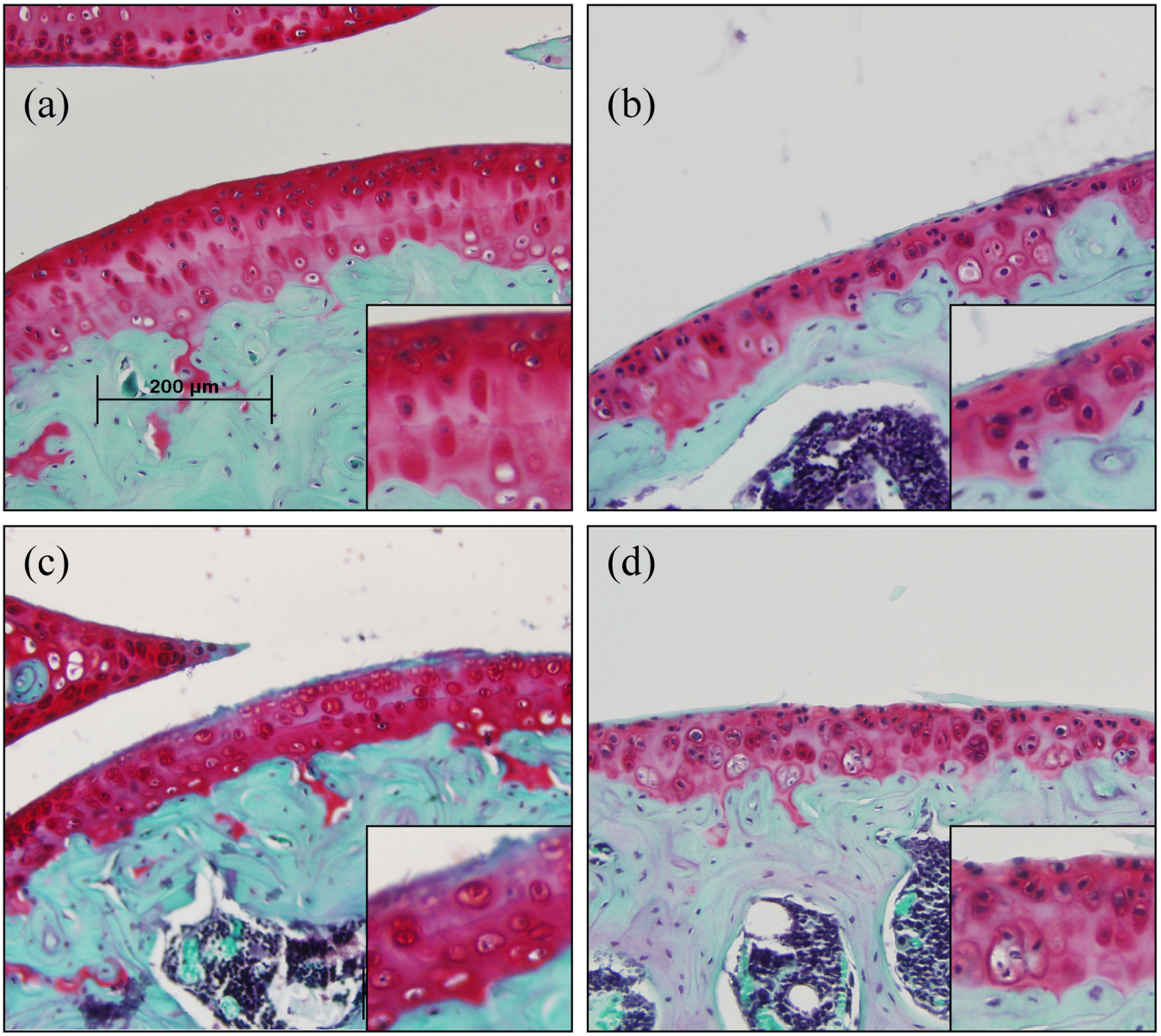

Fig. 2.

Paraffin-embedded tibial plateau sections: (a) wild-type; (b) $Bbs1^{M390R/M390R}$; (c) $Bbs2^{-/-}$; (d) $Bbs6^{-/-}$. Tissues are stained with the proteoglycan marker Safranin-O (red) and Fast Green FCF (blue). Knockin/knockout knees exhibit lower articular cartilage thickness and proteoglycan saturation, along with less mature appearing cell distribution than wild-type knees. 40× magnification insets.

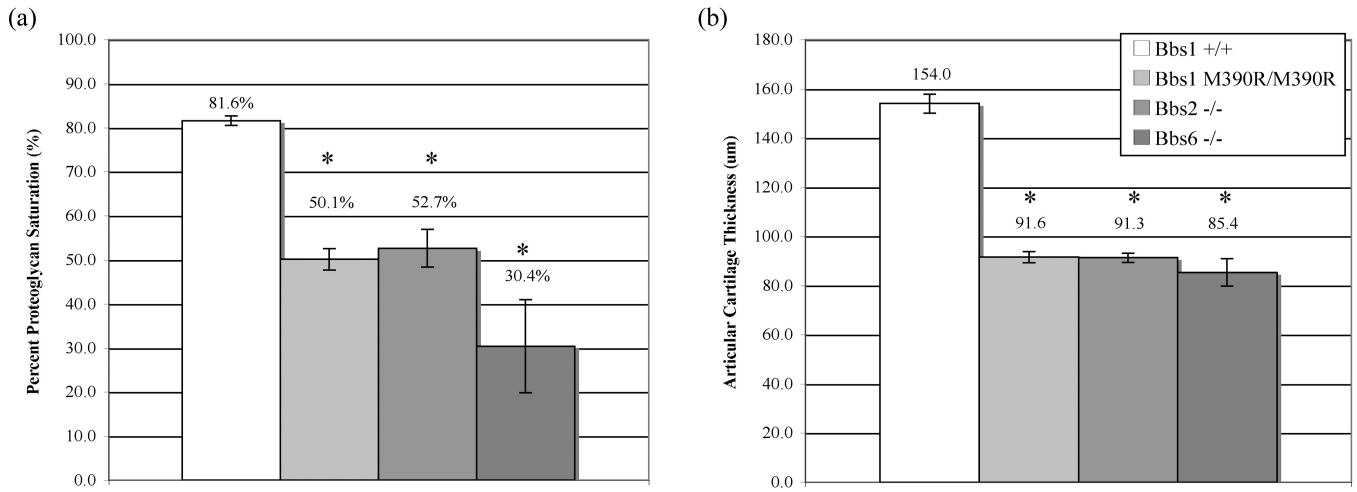

Fig. 3.

Histological comparison of tibial plateaus reveals that all knockin/knockout articular cartilage has significantly lower (a) proteoglycan saturation (percent) ($p<0.05$*) and (b) articular cartilage thickness (μm) ($p<0.05$*) than wild-type cartilage.

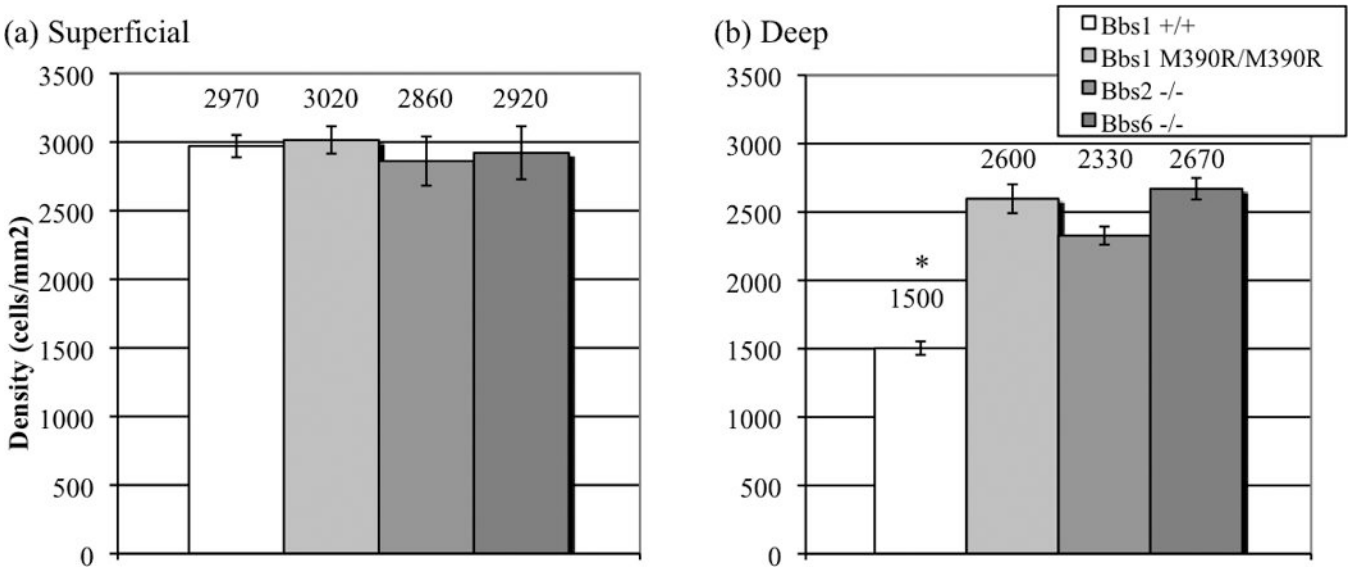

Fig. 4.

Cell density analysis of articular cartilage from tibial plateaus: (a) superficial layer (50% of articular cartilage area closest to joint surface); (b) deep layer (50% of articular cartilage area closest to subchondral bone). The superficial layer shows similar cell density in all mouse strains ($p>0.05$), however, the knockin/knockout cell density in the deep layer is significantly higher than in wild-type cartilage ($p<0.05$*), indicating a difference in cell distribution.

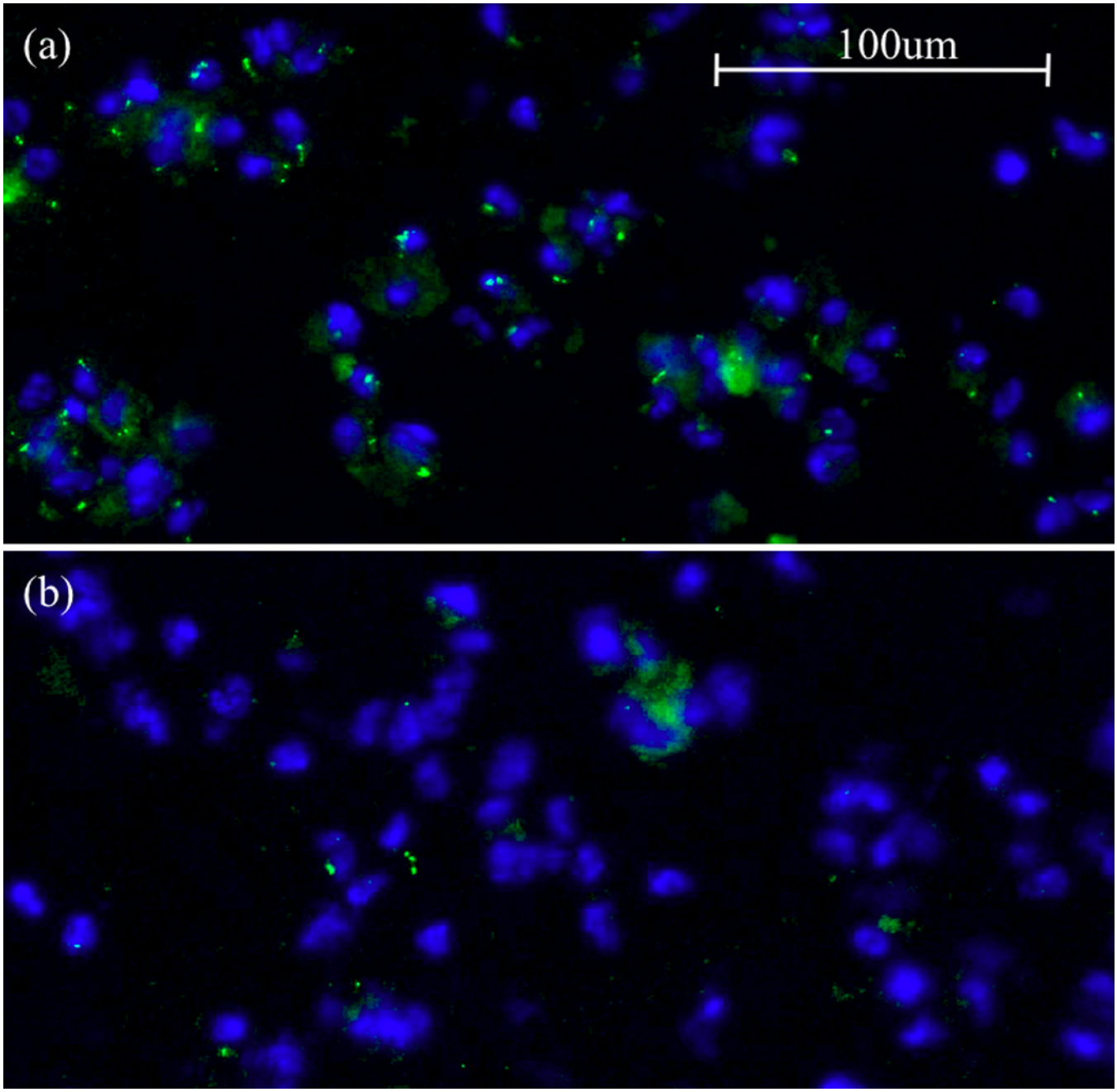

Fig. 5.

Sample immunofluorescence images of chondrocytic cilia in agarose plugs from day 1 of the agarose timecourse: (a) wild-type joints; (b) Bbs2$^{-/-}$ joints. Images display two-dimensional cross-sectional profiles containing the greatest number of visible cilia in the section; however, serial three-dimensional analysis was completed on all sections. Knockin/knockout cultures exhibit a visibly lower number of ciliated chondrocytes than wild-type cultures. Sections were stained with DAPI nuclear marker (blue) and antibody to acetylated α-tubulin (green).

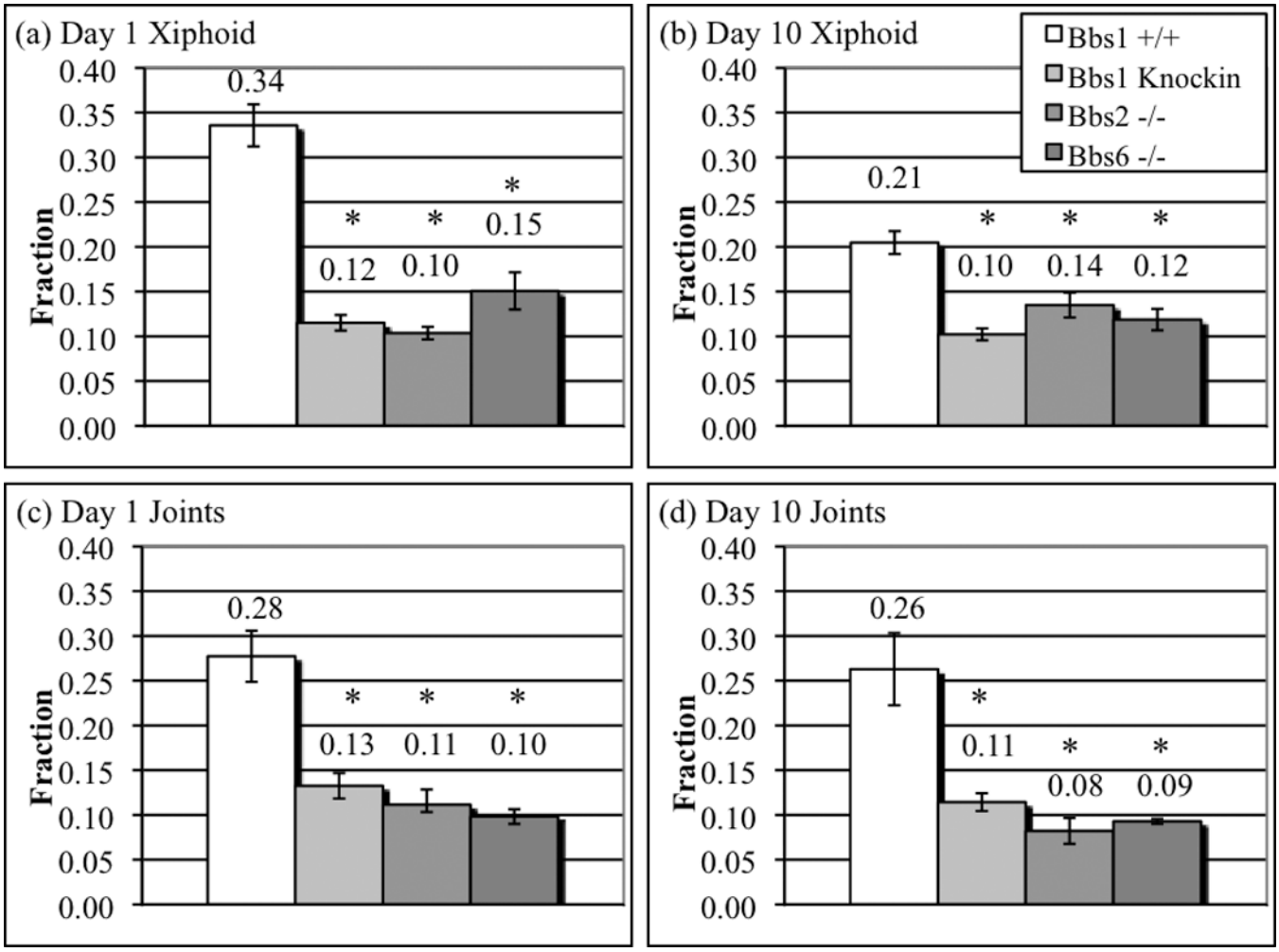

Fig. 6.

Fraction of chondrocytes with visible cilia in agarose timecourse cultures: (a) day 1 xiphoid; (b) day 10 xiphoid; (c) day 1 joints; (d) day 10 joints. In every agarose plug, knockin/knockout cultures had a significantly lower fraction of ciliated cells than wild-type cultures ($p<0.05$*). The fraction decreased over time from day 1 to 10 in most tissues, however, the knockin/knockout fraction remained significantly lower in both the xiphoid and joints. This analysis was performed by counting whole cells three-dimensionally with serial imaging of each section.